Original article

MOLECULAR METABOLISM

Peptidylglycine alpha-amidating monooxygenase is important in mice for beta-cell cilia formation and insulin secretion but promotes diabetes risk through beta-cell independent mechanisms

Yi-Chun Chen[1], Nils E. Bäck[2], Jenicia Zhen[1], Lena Xiong[1], Mitsuhiro Komba[1], Anna L. Gloyn[3], Patrick E. MacDonald[4], Richard E. Mains[5], Betty A. Eipper[5], C. Bruce Verchere[1,6,*]

ABSTRACT

Objectives: Carriers of *PAM* (peptidylglycine alpha-amidating monooxygenase) coding variant alleles have reduced insulinogenic index, higher risk of developing type 2 diabetes (T2D), and islets from heterozygous carriers of the *PAM* p.Asp563Gly variant display reduced insulin secretion. Exactly how global PAM deficiency contributes to hyperglycemia remains unclear. PAM is the only enzyme capable of converting glycine-extended peptide hormones into amidated products. Like neuropeptide Y (NPY), α-melanocyte stimulating hormone (αMSH), and glucagon-like peptide 1 (GLP-1), islet amyloid polypeptide (IAPP), a beta cell peptide that forms islet amyloid in type 2 diabetes, is a PAM substrate. We hypothesized that Pam deficiency limited to beta cells would lead to reduced insulin secretion, prevent the production of amidated IAPP, and reveal the extent to which loss of Pam in β-cells could accelerate the onset of hyperglycemia in mice.

Methods: PAM activity was assessed in human islets from donors based on their *PAM* genotype. We generated beta cell-specific *Pam* knockout (*Ins1*$^{Cre/+}$, *Pam*$^{fl/fl}$; β*Pam*KO) mice and performed islet culture, histological, and metabolic assays to evaluate the physiological roles of Pam in beta cells. We analyzed human IAPP (hIAPP) amyloid fibril forming kinetics using synthetic amidated and non-amidated hIAPP peptides, and generated hIAPP knock-in beta cell-specific *Pam* knockout (*hIAPP*$^{w/w}$ β*Pam*KO) mice to determine the impact of hIAPP amidation on islet amyloid burden, islet graft survival, and glucose tolerance.

Results: PAM enzyme activity was significantly reduced in islets from donors with the *PAM* p. Asp563Gly T2D-risk allele. Islets from β*Pam*KO mice had impaired second-phase glucose- and KCl-induced insulin secretion. Beta cells from β*Pam*KO mice had larger dense-core granules and fewer and shorter cilia. Interestingly, non-amidated hIAPP was less fibrillogenic *in vitro*, and high glucose-treated *hIAPP*$^{w/w}$ β*Pam*KO islets had reduced amyloid burden. Despite these changes in beta cell function, β*Pam*KO mice were not more susceptible to diet-induced hyperglycemia. *In vitro* beta cell death and *in vivo* islet graft survival remained comparable between *hIAPP*$^{w/w}$ β*Pam*KO and *hIAPP*$^{w/w}$ islets. Surprisingly, aged *hIAPP*$^{w/w}$ β*Pam*KO mice had improved insulin secretion and glucose tolerance.

[1]Department of Surgery, Faculty of Medicine, University of British Columbia & BC Children's Hospital Research Institute, 950 West 28th Avenue, Vancouver, BC, V5Z 4H4, Canada [2]Department of Anatomy, Faculty of Medicine, University of Helsinki, PO Box 63 (Haartmaninkatu 8), 00014 University of Helsinki, Finland [3]Department of Pediatrics, Division of Endocrinology & Diabetes and Department of Genetics, Stanford School of Medicine, Stanford Research Park, 3165 Porter Drive, Stanford, CA, 94304, USA [4]Department of Pharmacology and Alberta Diabetes Institute, 6-126C Li Ka Shing Centre for Health Research Innovation, Alberta Diabetes Institute, University of Alberta, Edmonton, AB, T6G 2E1, Canada [5]Department of Neuroscience, University of Connecticut Health Center, 263 Farmington Avenue, MC 3401, Farmington, CT, 06030-3401, USA [6]Centre for Molecular Medicine and Therapeutics, University of British Columbia, 950 West 28th Avenue, Vancouver, BC, V5Z 4H4, Canada

*Corresponding author. Departments of Surgery & Pathology and Laboratory Medicine, University of British Columbia & BC Children's Hospital Research Institute, 950 West 28th Avenue, Vancouver, BC, V5Z 4H4 Canada.

E-mails: yichen@bcchr.ca (Y.-C. Chen), nils.back@helsinki.fi (N.E. Bäck), jenicia.zhen@bcchr.ca (J. Zhen), mkomba@bcchr.ca (M. Komba), agloyn@stanford.edu (A.L. Gloyn), pmacdonald@ualberta.ca (P.E. MacDonald), mains@uchc.edu (R.E. Mains), eipper@uchc.edu (B.A. Eipper), bverchere@bcchr.ca (C.B. Verchere).
𝕏 (Y.-C. Chen), 𝕏 (C.B. Verchere)

Abbreviations: αMSH, α-melanocyte stimulating hormone; β*Pam*KO, Beta-cell-specific peptidylglycine alpha-amidating monooxygenase knockout; Cpe, carboxypeptidase E; GLP-1, glucagon-like peptide 1; HFD, high fat diet; hIAPP, human islet amyloid polypeptide; *hIAPP*$^{w/w}$, human islet amyloid polypeptide knock-in; IAPP, islet amyloid polypeptide; iβ*Pam*KO, inducible beta-cell-specific peptidylglycine alpha-amidating monooxygenase knockout; IPGTT, intraperitoneal glucose tolerance test; LFD, low fat diet; NPY, neuropeptide Y; Pam, peptidylglycine alpha-amidating monooxygenase; Pc1/3, prohormone convertase 1/3; Pc2, prohormone convertase 2; TRH, thyrotropin-releasing hormone; TUNEL, terminal deoxynucleotidyl transferase dUTP nick end labeling; Wt, wild-type

Received November 19, 2024 • Revision received March 10, 2025 • Accepted March 10, 2025 • Available online 20 March 2025

https://doi.org/10.1016/j.molmet.2025.102123

Conclusions: Eliminating *Pam* expression only in beta cells leads to morphological changes in insulin granules, reduced insulin secretion, reduced hIAPP amyloid burden and altered ciliogenesis. However, in mice beta-cell *Pam* deficiency has no impact on the development of diet- or hIAPP-induced hyperglycemia. Our data are consistent with current studies revealing ancient, highly conserved roles for peptidergic signaling in the coordination of the diverse signals needed to regulate fundamental processes such as glucose homeostasis.

Keywords Type 2 diabetes risk gene; Peptide hormone amidation; Insulin granules; Islet cilia; Islet amyloid polypeptide

1. INTRODUCTION

Genome-wide association studies have placed pancreatic beta cell dysfunction center stage in the pathogenesis of type 2 diabetes (T2D) [1]. Among the list of identified genes, peptidylglycine alpha-amidating monooxygenase (*PAM*) coding variants (rs78408340; c.1616C > G; p. Ser539Trp and rs35658696; c.1688 A > G; p.Asp563Gly, NM_000919.3) are associated with reduced insulinogenic index and altered risk of T2D [2–6], and donor islets from carriers of p.Asp563Gly alleles have reduced glucose-stimulated insulin secretion [7]. Interestingly, genetic variation at the *PAM* locus is also associated with hypertension, and the carriers of risk alleles display insulin resistance and low-density lipoprotein atherogenicity [8]. Loss-of-function variants in *PAM* are also enriched in subjects with pituitary hypersecretion [9,10]. It remains unclear whether diminished Pam function in beta cells is an important contributor to the development of T2D, and what cellular mechanisms lead to reduced insulin secretion in carriers of *PAM* T2D-risk alleles.

Pam is a bifunctional enzyme expressed in the diverse array of cells known to engage in peptidergic signaling [11]. Pam is the only enzyme known to amidate neuroendocrine peptides that have a carboxy-terminal glycine, creating peptide-amides [12] important for peptide stability and/or biological activity [13]. The importance of Pam extends beyond its enzymatic action [14]. Pam travels along secretory pathways, acts as a cargo receptor, and controls vesicle and membrane trafficking [15]. It has also been reported that a soluble Pam fragment released from endoproteolytic cleavage can enter the nucleus and control granule protein expression [16]. Pam can also play an essential role in ciliogenesis [17]. The expression and activity of Pam fluctuates with nutrients and extracellular stimuli [18–21], highlighting Pam's roles in fine-tuning cellular processes to maintain behavioral or metabolic homeostasis.

We previously reported that *Pam* global heterozygous knockout mice failed to gain more weight nor become more hyperglycemic, even after consuming a high fat diet [20]. Although not sufficient to maintain hypothalamic levels of thyrotropin-releasing hormone (TRH) [22], the remaining 50% Pam activity did not result in lowered amidated islet amyloid polypeptide (IAPP) levels in islets from *Pam* heterozygous mice [20]. The regulation of glucose homeostasis involves a vast number of neuroendocrine peptides; while the synthesis of many of these peptides requires Pam, the synthesis of others does not [23]. To define the role of Pam in beta cells and understand the effect of eliminating Pam function in this single cell type on glucose homeostasis, we generated beta-cell specific *Pam* knockout mice.

Human IAPP (hIAPP) self-aggregates to form amyloid fibrils that contribute to beta cell death and islet inflammation. Since post-translational modifications and/or mutations in hIAPP could alter amyloid fibril-forming capacity [24] and Pam is essential for IAPP amidation [20], we used beta cell-specific *Pam* knockout hIAPP knock-in mice to test the hypothesis that Pam deficiency would influence islet amyloid burden, islet graft survival, and glucose intolerance.

2. MATERIAL AND METHODS

2.1. Human pancreas samples

Human pancreas tissue was obtained from deceased donors under ethical approval from the Human Research Ethics Board of the University of Alberta (Pro00013094, Pro00001754) and with informed written consent. Tissue biopsies from the pancreas tail were formalin fixed, and paraffin embedded (FFPE), and cut into 5 μm sections for histological analysis. DNA samples were extracted from acinar tissue and genotyped on Illumina Infinium Omni2.5Exome-8 BeadChip arrays (Illumina, San Diego, CA, USA) to identify carriers of the rs35658696 *PAM* T2D-risk allele. Age-, BMI-, and sex-matched non-carriers of *PAM* T2D risk alleles were selected as controls. Donor characteristics are listed in Supplementary Table 1; further information can be found at www.humanislets.com.

2.2. Rodent studies

Beta-cell-specific *Pam* knockout (β*Pam*KO) and inducible beta-cell-specific *Pam* knockout (iβ*Pam*KO) mice were generated by crossing $Pam^{fl/fl}$ mice [25] with $Ins1^{Cre/+}$ mice [26] or MIP-CreERT^{1Lphi} mice [27]. As human but not mouse IAPP aggregates to form amyloid fibrils, human IAPP knock-in mice ($hIAPP^{w/w}$) [28] were crossed to β*Pam*KO mice to study the impact of hIAPP amidation on amyloid fibril formation (mouse information listed in Supplementary Table 2), For metabolic studies, β*Pam*KO mice received either a low-fat diet (LFD; 10% fat; #D12450H; Research Diets, New Brunswick, NJ, USA), or a high-fat diet (HFD; 45% fat, #D12451; Research Diets), starting from 10 weeks of age. Body weight and fasting blood glucose levels were measured biweekly for 20 weeks, and intraperitoneal glucose tolerance tests (IPGTT) were performed at 16 weeks after diet treatment. Tamoxifen was administered orally to 8 wk-old $Pam^{fl/fl}$ x MIP-CreERT^{1Lphi}, $Pam^{fl/fl}$, and MIP-CreERT^{1Lphi} mice to induce Cre recombinase expression. At 9 weeks after tamoxifen treatment, IPGTT was performed on iβ*Pam*KO and control mice. In addition to IPGTT, plasma from $hIAPP^{w/w}$ mice and *hIAPP* knock-in β*Pam*KO mice during oral glucose tolerance tests was also collected to measure insulin levels by commercial ELISA kits (#80-INSMR-CH10, Alpco Diagnostics, Salem, NH, USA). All metabolic assays were performed in both sexes in a blinded fashion.

For islet transplantation, wild-type (*WT*) C57/BL6 mice received multiple low-dose streptozotocin (35 mg/kg body weight, daily i. p. for 5 days; #S0130-500 MG, Sigma–Aldrich, St. Louis, MO, USA) injections to induce hyperglycemia. Islets from *WT*, $hIAPP^{w/w}$, and $hIAPP^{w/w}$ β*Pam*KO mice were transplanted into the anterior eye chamber of hyperglycemic *WT* mice, and diabetes incidence (blood glucose level >20 mM) post-transplant was documented.

Mice were kept under regular light/dark cycles and had access to food and water ad libitum. All procedures were approved by the Animal Care and Use Committee at the University of British Columbia.

2.3. Islet studies

Mouse pancreatic islets were isolated and cultured as described [29]. Insulin secretion dynamics from *WT* and β*Pam*KO mouse islets were

analyzed using the BioRep Perifusion System V5. For measurement of other islet hormones, *WT* and β*Pam*KO islets were statically incubated in low (1 mM) and high (11 mM) glucose buffer, and glucagon and somatostatin levels measured using commercial ELISA kits (proinsulin: #10-1232-01, Mercodia, Uppsala, Sweden; glucagon: #10-1281-01, Mercodia; somatostatin: #EK-060-03, Phoenix Pharmaceuticals, Burlingame, CA, USA).

2.4. Insulin granule analysis

Freshly isolated mouse islets were fixed with 2.5% glutaraldehyde, osmicated, dehydrated and embedded in Epon. Sections were post-stained with uranyl acetate and lead citrate. Each section contained several islets which were systematically photographed with 4000× magnification at fixed intervals with a random start using a Jeol JEM-1400 electron microscope equipped with a Gatan Orius SC 1000 B bottom mounted CCD-camera. This unbiased sampling of all parts of the cytoplasm allowed morphometric analysis of the cytoplasmic volume fraction occupied by specific organelles [30], which was quantified with the Stereology function in Microscopy Image Browser [31]. Transection areas of immature ($n > 260$ per genotype group) and mature secretory granules ($n > 1800$ per genotype group), length of plasma membrane and distances between plasma membrane and secretory granule membranes were analyzed with Fiji [32]. Of note, as most mature secretory granules are elliptical rather than round, area was measured instead of diameter. The measured distances between plasma membrane and secretory granule membranes are affected by the fact that most granules are not sectioned through their middle.

2.5. Immunostaining

Islet cilia [33], amyloid burden [20], and islet morphology [34] were analyzed as previously described. hIAPP oligomers were detected in islet cryosections via conventional immunostaining protocols [35], using antibodies and reagents listed in Supplementary Table 3. Beta cell death was analyzed via Fixable Viability Dye staining (#65-0867-14, Thermo Fisher Scientific, Waltham, MA, USA) and terminal deoxynucleotidyl transferase dUTP nick end labeling (TUNEL) assay (#11684795910, Roche, Basel, Switzerland) following manufacturers' protocols.

2.6. Image acquisition and analysis

Islet cilia images were taken at 40× magnification using a Leica TCS SP5 confocal microscope (Leica Microsystems, Wetzlar, Hesse, Germany). 20–30 z-stack images from deconvoluted image sets were selected and combined via maximal intensity projection using Huygens Professional software (Version 18.04, Scientific Volume Imaging, Hilversum, Netherlands). Cilia length and number were quantified using an Image J plug-in module CiliaQ [36]. Islet images were taken using Leica TCS SP5 confocal microscope and Olympus BX61 automated fluorescence and transmittance upright microscope (Olympus, Shinjuku, Tokyo, Japan). Islet amyloid, oligomers, TUNEL, and Fixable Viability Dye staining were analyzed using CellProfiler software (Version 4) [37]. Amidated IAPP, non-amidated IAPP, and insulin expression levels, as well as islet cell type composition, were quantified using QuPath software (Version 0.5.1) [38].

2.7. hIAPP aggregation assays

hIAPP peptides (amino acid sequences listed in Supplementary Table 2) were custom-ordered from Bio-Synthesis (Lewisville, TX, USA), dissolved in hexafluoro-2-propanol, lyophilized, and stored at −20C. Immediately prior to the experiments, lyophilized peptides were dissolved in PBS (final concentration 15 μM) at room temperature for 24 h and analyzed via negative staining using a transmission electron microscope with technical assistance from UBC Bioimaging Facility (Hitachi H7600 transmission electron microscope, Chiyodaku, Tokyo, Japan); or incubated with 10 μM thioflavin T (#T3516, MilliporeSigma, Burlington, MA, USA) in a thioflavin T assay buffer (10 mM Tris–HCl, 100 mM NaCl, 0.1% Triton X-100, pH = 7.4) at 37 °C with fluorescence kinetics recorded via a Tecan Infinite 200 Pro plate reader (Tecan Group Ltd, Männedorf, Switzerland).

2.8. qRT-PCR

Islet mRNA was isolated using PureLink RNA Micro Kit (#12183016, Thermo Fisher Scientific), converted to cDNA using a SuperScript VILO cDNA Synthesis kit (#11754050, Thermo Fisher Scientific), and quantified through SYBR Green-based quantitative real-time PCR (qRT-PCR) approach using Fast SYBR™ Green Master Mix (#4385612, Applied Biosystems, Waltham, MA, USA), and a ViiA7 Real-Time Thermocycler (Applied Biosystems) as previously described [20].

2.9. Statistical analysis

Statistical analyses were performed using Prism software (Version 10, GraphPad, La Jolla, CA, USA). All data are presented as mean ± SEM, and the detailed statistical methods used are indicated in the figure legends.

3. RESULTS

3.1. Reduced IAPP amidation in *PAM* p.Asp563Gly T2D-risk allele carriers

Recombinant PAM p.Asp563Gly protein has reduced enzyme activity *in vitro* and reduced activity in serum [7,9,39]. To evaluate whether *PAM* T2D-risk allele carriers have reduced islet PAM activity, we performed immunostaining to analyze amidated (Figure 1A, upper panels) and non-amidated IAPP levels (Figure 1A, lower panels) in pancreatic sections from *PAM* p.Asp563Gly T2D-risk allele carriers (heterozygous) and age- and BMI- matched non-carrier donors (donor characteristics are described in Supplementary Table 1). Amidated IAPP levels in insulin-positive cells were significantly reduced in *PAM* T2D-risk allele carriers (Figure 1B), suggesting reduced PAM enzyme activity in the islet. Non-amidated IAPP and insulin expression levels, on the other hand, were comparable between carriers and non-carriers of the *PAM* T2D-risk allele (Figure 1C,D).

3.2. Altered beta-cell insulin granule morphology in β*Pam*KO mice

To reveal the role of beta-cell Pam in the development of diabetes, we generated beta-cell specific *Pam* knockout (β*Pam*KO, $Pam^{fl/fl}$ x $Ins1^{Cre/+}$) mice. Pam was deleted in beta cells, but unaffected in alpha cells in β*Pam*KO mice (Figure 1E).

Since eliminating the expression of Pam in atrial myocytes reduced their ability to produce secretory granules, we used electron microscopy to compare the volume fraction occupied by various organelles in the beta cells of wild-type and β*Pam*KO mice [40]. Beta cell-specific Pam deletion had no effect on the volume occupied by secretory granules, golgi stacks, lysosomes, or endoplasmic reticulum (Figure 2A–C).

The secretory granules of beta cells undergo a maturation process, with immature secretory granules readily distinguished from mature secretory granules (Figure 2D). Immature secretory granules were of similar size in β*Pam*KO and wild-type beta cells. During maturation, the transection area of secretory granules in wild-type cells decreased by 12.7% ($p < 0.001$); no size change occurred during granule maturation in β*Pam*KO beta cells (Figure 2D), suggesting that Pam

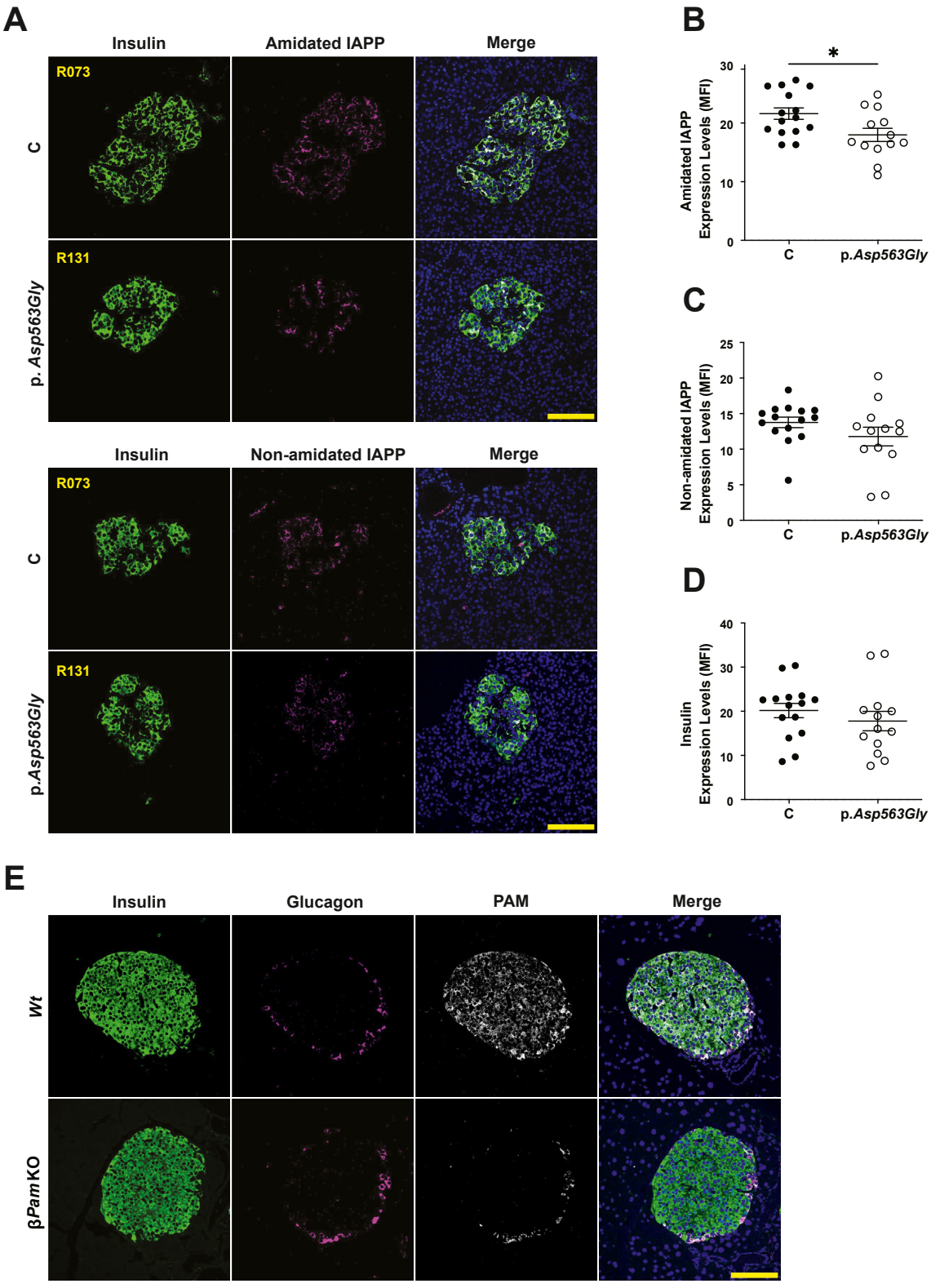

Figure 1: Reduced islet PAM activity in p.Asp563Gly-PAM variant carriers.
(A) Representative immunofluorescence images of human pancreatic sections of control (C) and p.Asp563Gly-PAM variant carriers (p.*Asp5*63Gly) with antibodies that target insulin and amidated IAPP (upper panels), or insulin and non-amidated IAPP (lower panels). **(B–D)** Quantitative analysis of amidated IAPP, non-amidated IAPP, and insulin expression levels in islets of control and *PAM* variant carriers. MFI, mean fluorescence intensity. **(E)** Representative immunofluorescence images of islets from wild-type (*Wt*) and beta cell-specific *Pam* knockout (β*Pam*KO) mice using antibodies that target insulin, glucagon and Pam. Scale bar = 100 μm. Data are presented as mean ± SEM, $*p < 0.05$.

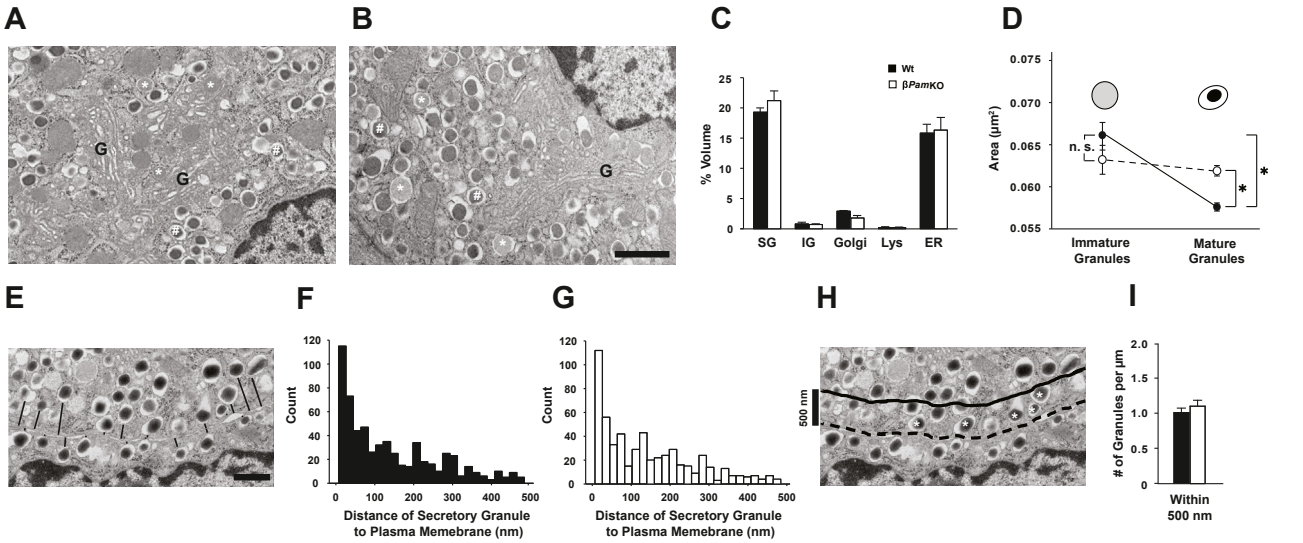

Figure 2: Altered organelle morphology in *Pam* knockout beta cells.
In both *Wt* **(A)** and β*Pam*KO **(B)** beta cells, Golgi stacks (G) were surrounded by mature secretory granules: * denotes typical immature secretory granules; # denotes typical mature secretory granules. Scale bar = 1 μm. **(C)** The cytoplasmic volume fractions of mature secretory granules (SG), immature secretory granules (IMG), Golgi stacks, lysosomes (Lys) and endoplasmic reticulum (ER) are similar in *Wt* (black columns) and β*Pam*KO (white columns) beta cells. n = 4 mice; 18 and 26 islets per genotype, 40 images per mouse, data are expressed as mean ± SE. **(D)** Transection areas in μm^2 of immature secretory granules and mature secretory granules in *Wt* beta cells (black circles) and β*Pam*KO beta cells (empty circles) (schematically depicted above). n > 260 immature secretory granules per genotype, and n > 1800 mature secretory granules per genotype. Data are expressed as mean ± SE. n. s. = not statistically significant; * = $p < 0.001$. Representative micrograph **(E)** and quantitative analysis of distances between the plasma membrane and the closest membrane of peripheral secretory granules in *Wt* **(F)** and β*Pam*KO **(G)** beta cells. n > 560 measurements per genotype. Scale bar = 500 nm. Representative micrograph **(H)** of readily releasable granules (situated within the peripheral zone, 500 nm from the plasma membrane, which is marked by the dashed line) and quantitative analysis **(i)** of numbers of secretory granules situated within the peripheral zone in *Wt* (black column) and β*Pam*KO (white column) beta cells. n > 730 granules per genotype. Vertical scale bar = 500 nm. Data are expressed as mean ± SE. *$p < 0.05$.

promotes insulin granule condensation. The distance of insulin granules from the plasma membrane is also an indicator of granule maturation [41]. We found that the spatial distribution of insulin granules was comparable in β*Pam*KO and wild-type beta cells (Figure 2E–G). Secretory granules located in the peripheral zone (within 500 nm of the plasma membrane) of the cytoplasm are thought to represent the readily releasable pool of secretory granules (Figure 2H); quantification revealed no difference in this number (Figure 2I). Our data suggest that Pam likely facilitates the condensation and refilling of secretory granules [42].

3.3. Impaired islet hormone secretion in β*Pam*KO islets

Previous reports showed that islets from carriers of the p.Asp563Gly-PAM T2D-risk allele have disrupted insulin secretion, and *PAM* knockdown in EndoC-βH1 cells led to significantly reduced insulin content with concomitant impairments in glucose-stimulated insulin secretion [7]. We analyzed insulin secretion dynamics using perifused islets from *Wt* and β*Pam*KO mice (Figure 3A). In this way we could distinguish first-from second-phase secretion of insulin and compare the stimulatory effect of glucose to that of depolarization in response to elevated KCl. First-phase glucose-stimulated insulin secretion was comparable in *Wt* and β*Pam*KO islets (Figure 3B). By contrast, second-phase glucose-stimulated and KCl-stimulated insulin secretion were both impaired in β*Pam*KO islets (Figure 3C,D). Our finding of impaired second-phase insulin secretion in β*Pam*KO islets is compatible with a role for Pam in insulin granule biogenesis [7].

To see if the lack of beta-cell *Pam* expression alters the function of other islet endocrine cells, we assessed glucagon and somatostatin secretion in islets from in β*Pam*KO and Wt mice. Both glucagon secretion and somatostatin secretion were disrupted in β*Pam*KO islets (Figure 3E–H), with modest reductions in glucagon and somatostatin secretion in the presence of 1 mM but not 11 mM glucose. While glucagon content was unaltered (Figure 3F), the somatostatin content of β*Pam*KO islets was diminished compared to Wt (Figure 3H).

3.4. Reduced islet cilia length and density in β*Pam*KO mice

Proper islet hormone secretion requires functional beta-cell cilia [43] and Pam is involved in cilia formation in other cell types [17]. To determine whether reduced insulin secretory capacity in β*Pam*KO islets could stem from defective beta-cell cilia, we performed immunostaining and quantitative analysis of cilia in islets isolated from *Wt* and β*Pam*KO mice (Figure 4A). Both the length and density of islet cilia were reduced in β*Pam*KO mice (Figure 4B,C). These data raise the possibility that impaired cilia formation associated with the lack of Pam expression in beta cells could contribute to altered islet-cell communication and hormone secretion [43].

The percentage of beta cells, but not alpha or delta cells, was reduced in β*Pam*KO islets (Figure 4D–G). Our data fit with previous findings that primary cilia are important for development of normal islet cell populations [44]. Overall pancreas beta cell area was comparable in *Wt* and β*Pam*KO mice (Figure 4H,I), indicating that extreme ciliopathy is required to disrupt beta cell mass. Together, these data suggest that Pam mediates islet hormone secretion and islet primary cilia formation.

3.5. β*Pam*KO mice do not display accelerated development of glucose intolerance after high fat diet challenge

To test whether a total lack of *Pam* expression exclusively in beta cells is sufficient to drive the development of diabetes, we measured metabolic parameters in β*Pam*KO and littermate controls. To better mimic the effects of *Pam* haploinsufficiency, both β*Pam*HET and *Wt* mice were

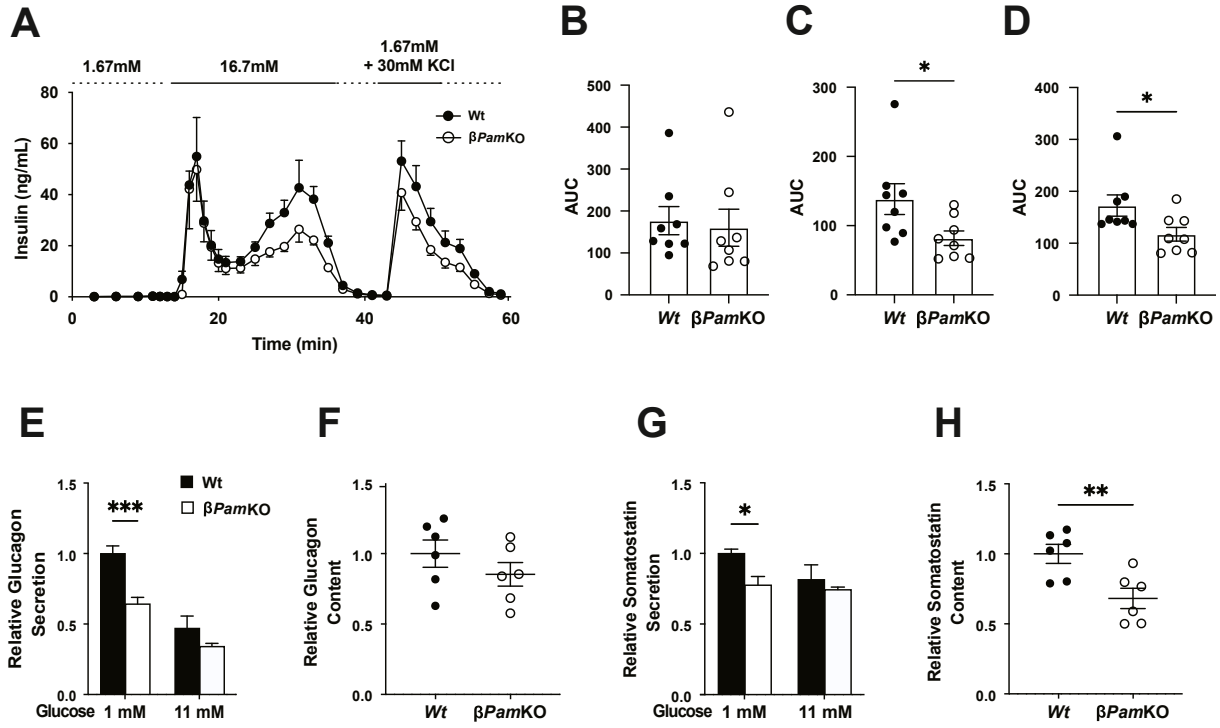

Figure 3: Reduced islet hormone secretion in beta-cell *Pam* knockout islets.
(A) Perifused islets were used to examine insulin secretion dynamics in *Wt* and β*Pam*KO mice. Islets were exposed to 1.67 mM glucose for 15 min (basal secretion), to 16.7 mM glucose for 20 min and then to 1.67 mM glucose with 30 mM KCl for 10 min; samples were collected every minute, with selected timepoints analyzed by insulin ELISA. Area-under-curve (AUC) analysis of first-phase **(B)**, second-phase **(C)**, and KCl-stimulated **(D)** insulin secretion in islets from *Wt* and β*Pam*KO mice. **(E, F)** Glucagon secretion and glucagon content, and **(G, H)** somatostatin secretion and somatostatin content of *Wt* (filled bar) and β*Pam*KO (empty bar) islets. Data are presented as mean ± SEM. n ≥ 3 mice per group, $*p < 0.05$.

examined. Male β*Pam*KO, β*Pam*HET, and *Wt* mice had similar baseline body weights and fasting blood glucose levels (Figure 5A,B). When kept on a low-fat diet (LFD) for 20 weeks, all three groups of male mice gained a similar amount of weight (Figure 5A), had comparable fasting glucose levels (Figure 5B), and responded in a similar manner to intraperitoneal glucose (Figure 5C). When kept on a high-fat diet (HFD) for 20 weeks, all three groups of male mice gained more weight than they did on the LFD (Figure 5D vs. 5A), had similarly elevated fasting blood glucose levels (Figure 5E vs. 5B), and exhibited diminished ability to respond to intraperitoneal glucose (Figure 5F vs. 5C).

The same paradigm was used to evaluate female β*Pam*KO, β*Pam*HET, and *Wt* mice. In female mice, as in males, body weight (Figure 5G) and fasting blood glucose levels (Figure 5H) remained similar over the 20 weeks of LFD. Intraperitoneal glucose tolerance tests carried out after 20 weeks on LFD revealed no differences (Figure 5I). Although female mice were less susceptible than male mice to HFD-induced metabolic abnormalities (Figure 5D—F vs. 5J–5L), β*Pam*KO, β*Pam*HET, and *Wt* mice displayed similar weight gain, fasting blood glucose levels, and glucose tolerance after 20 weeks of HFD treatment.

To account for possible compensatory effects that might mitigate the impact of lifelong *Pam* deficiency, we generated inducible beta cell-specific Pam knockout mice (iβ*Pam*KO; $Pam^{fl/fl}$ x MIP-CreERT^{1Lphi}). Levels of islet Pam mRNA in iβ*Pam*KO mice were reduced to a fifth of controls 2 weeks after tamoxifen treatment (Figure 5M). Wt and iβ*Pam*KO mice displayed similar body weight and fasting glucose levels (data not shown). At 17 weeks of age, 9 weeks after beta-cell Pam deletion, glucose tolerance tests were carried out on male and female *Wt* and iβ*Pam*KO mice. While male iβ*Pam*KO and Wt mice produced similar responses (Figure 5N,O), very modest glucose intolerance was observed in female iβ*Pam*KO mice (Figure 5P,Q). Our results suggest that, despite the impact of beta-cell *Pam* deletion on cilia formation and insulin secretion, compensatory control mechanisms available *in vivo* ensure that glucose metabolism can be maintained, even in the presence of the metabolic stress of HFD.

3.6. Amidation of human IAPP enhances both its aggregation and amyloidogenic activity

In both human and mouse beta cells, endoproteolytic cleavage of proIAPP, followed by exoproteolytic cleavages by carboxypeptidase E (Cpe) produces peptidylglycine intermediates that are converted by Pam into mature IAPP, which terminates with a C-terminal Tyr-NH_2 (Figure 6A). Human islet amyloid polypeptide (hIAPP) is prone to self-aggregation and hIAPP oligomers and islet amyloid fibrils (schematic illustration of hIAPP aggregation pathway shown in supplementary Figure 1a) may contribute to beta-cell death and islet inflammation [24]. Unlike hIAPP, mouse IAPP has 3 prolines localized within residues 20 and 29 of its amyloidogenic region, which prevents it from spontaneous self-aggregation. Incomplete hIAPP processing, amino acid substitutions, and post-translational modifications have all been shown to impact IAPP amyloid fibril-forming kinetics and morphology [45—49]. The effect of hIAPP amidation on aggregation was assessed using synthetic peptides and a thioflavin T-binding assay (Figure 6B) [47]. Fluorescence intensity increased rapidly in the presence of amidated hIAPP (hIAPP-amide, magenta) while non-amidated hIAPP (hIAPP-Gly, grey) had no effect (Figure 6B), demonstrating an essential role for C-terminal amidation in hIAPP fibril formation. Intermediate-hIAPP-amide

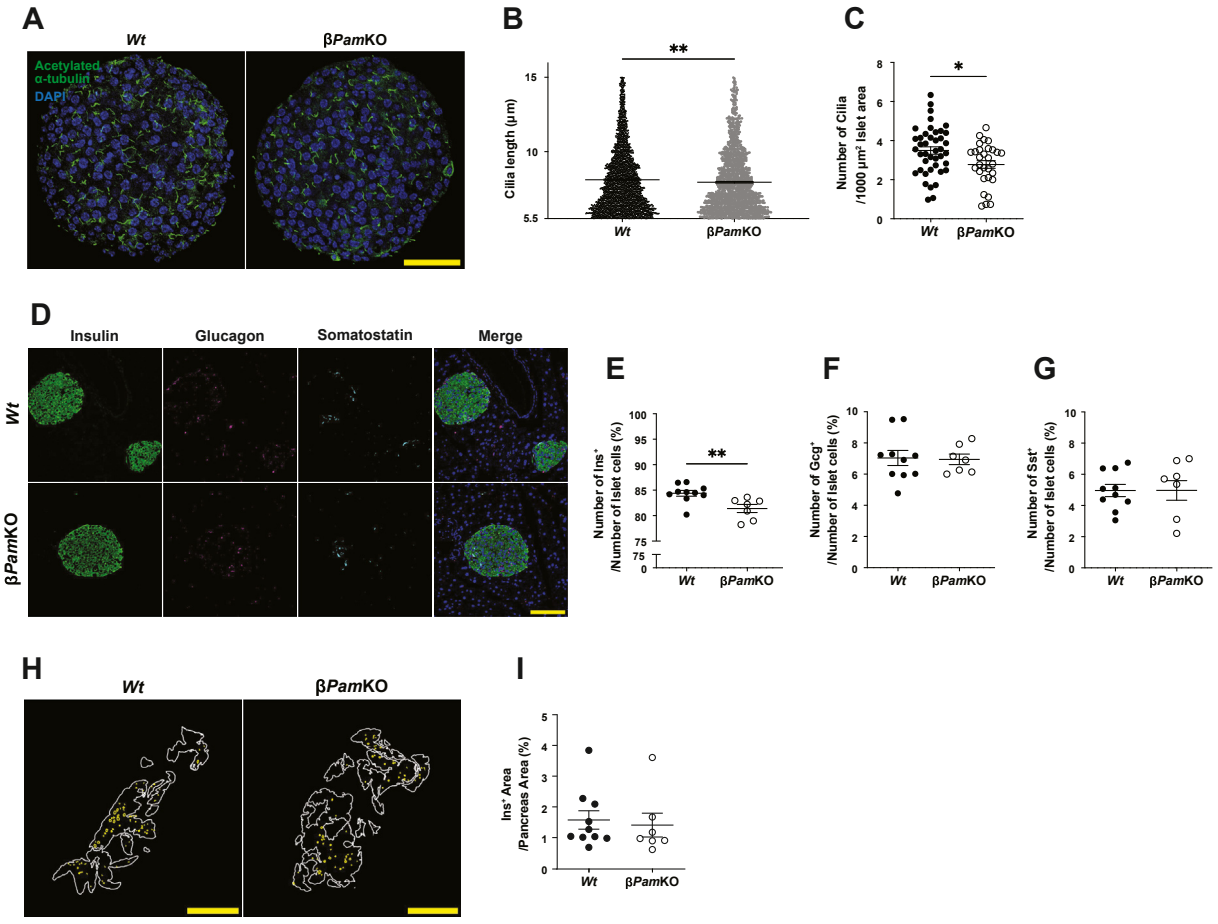

Figure 4: Altered primary cilia and islet cell distribution in beta-cell *Pam* knockout islets.
(A) Representative immunofluorescence images of primary cilia in *Wt* and β*Pam*KO islets. Scale bar = 50 µm Quantitative analysis of cilia length **(B)** and density **(C)** in *Wt* and β*Pam*KO islets. In total, 12086 cilia from 42 islets from 4 Wt mice, and 6239 cilia from 30 islets from 4 β*Pam*KO mice were analyzed. **(D)** Representative immunofluorescence images of islet cell distribution in *Wt* and β*Pam*KO mice. Scale bar = 100 µm **(E–G)** Percentage of insulin-positive (Ins^+), glucagon-positive (Gcg^+), and somatostatin-positive (Sst^+) cells in islets of Wt and β*Pam*KO mice. Each dot represents average percentage of Ins+, Gcg+, or Sst+ cells in islets from n = 10 (Wt) and 7 (βPamKO) mice. Representative tiled immunofluorescence images (scale bar = 5 mm) **(H)** and quantitative analysis of insulin-positive cells in the pancreas of *Wt* (n = 10) and β*Pam*KO (n = 7) mice **(I)**. Data are presented as mean ± SEM. $^*p < 0.05$.

(blue) produced slower aggregation kinetics than hIAPP-amide; like hIAPP-Gly, intermediate-hIAPP-Gly (brown) and pro-hIAPP (crimson) were ineffective in forming amyloid fibrils (Figure 6B). As expected, mouse IAPP-amide (mIAPP-amide) (black) did not form fibrils and was used as a negative control along with buffer control (empty circle). As beta cells have heterogeneous peptide processing capacity [50], differentially processed forms of hIAPP likely co-exist in beta cells and in the islet microenvironment. While amidated mature hIAPP supported rapid fibril formation (Figure 6C, magenta), co-incubation of non-amidated and amidated hIAPP revealed that that non-amidated hIAPP prevents islet amyloid fibril formation (Figure 6C, brown and gray).

To verify the results obtained using thioflavin T-binding kinetics and gain insight into hIAPP fibril structure, we captured transmission electron micrograph (TEM) images after hIAPP peptides had been kept in PBS for 24 h at room temperature. In keeping with results from the thioflavin T assay, hIAPP-Gly aggregates were amorphous (Figure 6D), unlike the long fibrils formed by hIAPP-amide (Figure 6D). Intermediate-hIAPP-amide yielded shorter fibrils while intermediate-hIAPP-Gly and pro-hIAPP did not stimulate fibrillation.

To evaluate the effects of hIAPP amidation on amyloid deposition *in situ*, we generated a model in which we could control the amidation of hIAPP in beta cells. To do so, we generated hIAPP knock-in, beta cell-specific *Pam* knock-out ($hIAPP^{W/W}$ β*Pam*KO) mice. As predicted, thioflavin S staining of amyloid fibrils in islets from $hIAPP^{W/W}$ β*Pam*Wt mice revealed the development of islet amyloid after prolonged culture in high glucose media [51]. In keeping with our studies using synthetic peptides, islets from Pam-deficient, $hIAPP^{W/W}$ β*Pam*KO mice exhibited significantly reduced islet amyloid deposition (Figure 6E,F). It has been proposed that pre-fibrillar hIAPP oligomers are more toxic to beta cells [52]; however, despite the presence of increased oligomeric aggregates as assessed by A11 staining (Supplementary Figure 1b and 1c), we found no evidence of increased cell death in cultured $hIAPP^{W/W}$ β*Pam*KO islets (Supplementary Figure 1d and 1e).

We also investigated whether reduced PAM catalytic activity results in reduced islet amyloid burden in humans, by performing thioflavin S staining in human pancreatic sections from carriers and matched non-carriers of the *PAM* T2D-risk allele (p.Asp563Gly) (Figure 6G). Of note, all donors studied were heterozygous and therefore retained partial peptide amidation capacity (Figure 1B). We found no significant difference in the percentage of thioflavin S-positive islet area (Figure 6H), nor thioflavin S-positive islet number (Figure 6I) between control and p.Asp563Gly-*PAM* variant carriers.

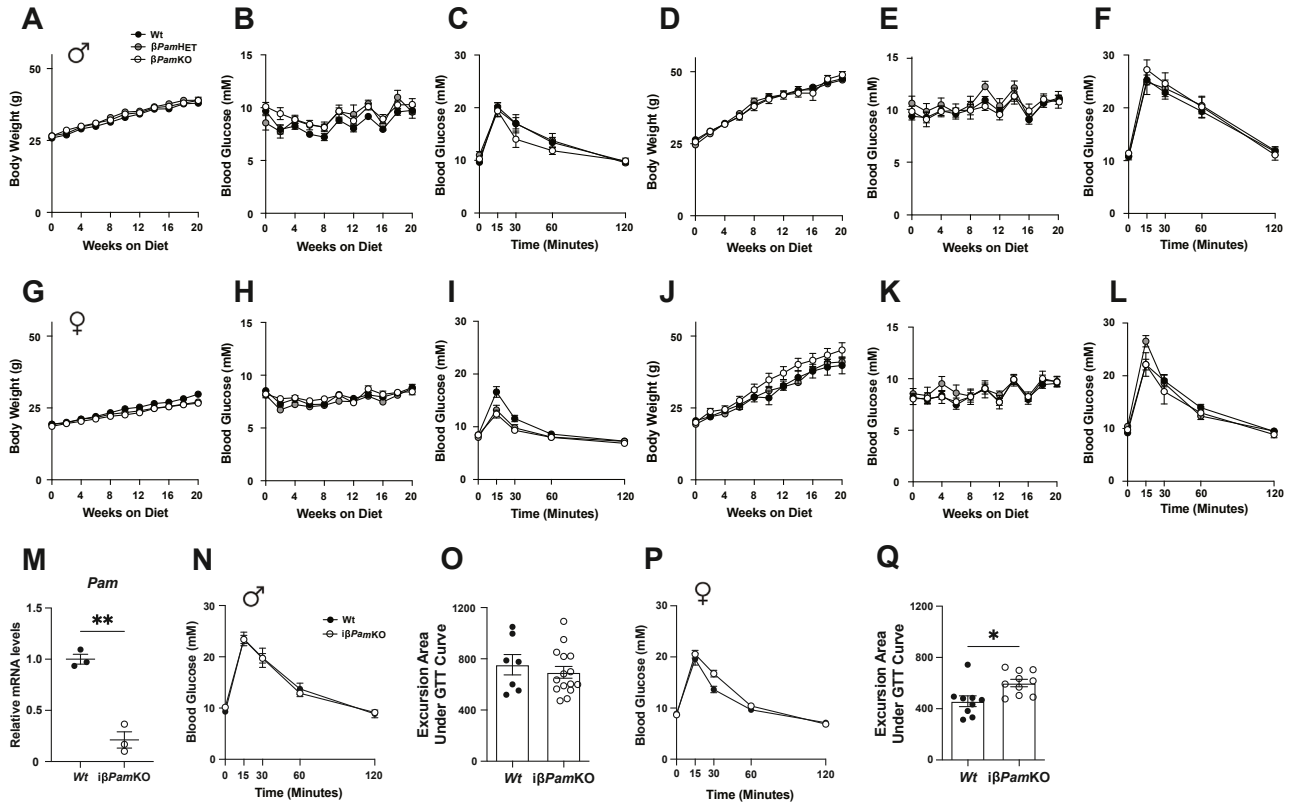

Figure 5: Beta-cell *Pam* knockout mice do not display impaired glucose tolerance.
Male *Wt* (filled black circle), beta cell specific Pam heterozygous knockout (β*Pam*HET, filled grey circle), and β*Pam*KO (empty circle) mice were fed a 10% fat diet **(A—C)** or a 45% fat diet **(D—F)** for 20 weeks, their body weights **(A, D)** and fasting blood glucose levels **(B, E)** were monitored every two weeks. At 16 weeks post-diet treatment, intraperitoneal glucose tolerance test (IPGTT) was performed **(C, F)**. Female *Wt*, β*Pam*HET, and β*Pam*KO mice were fed a 10% fat diet **(G—I)** or a 45% fat diet **(J—I)** for 20 weeks, their body weights **(G, J)** and fasting blood glucose levels **(H, K)** were monitored every two weeks. At 16 weeks post-diet treatment, IPGTT was performed **(I, L)**. **(M)** Islet Pam transcript levels were analyzed at 2 weeks after tamoxifen treatment. IPGTT was performed on male **(N, O)** and female **(P, Q)** inducible beta cell-specific Pam knockout (iβ*Pam*KO) mice at 9 weeks after tamoxifen treatment, and the area under the glucose excursion curve was analyzed. Data are presented as mean ± SEM. n ≥ 7 mice per group, $*p < 0.05$.

To study whether the presence of non-amidated hIAPP accelerates islet failure in the presence of hyperglycemia, we transplanted pancreatic islets from *hIAPP*$^{W/W}$ β*Pam*KO or control (*hIAPP*$^{W/W}$ β*Pam*Wtor *Wt*) mice into the anterior chamber of the eye of streptozotocin-induced diabetic mice (Figure 6J). While hyperglycemia was successfully reversed upon islet transplantation, mice that received islets from *hIAPP*$^{W/W}$ β*Pam*KO, *hIAPP*$^{W/W}$ β*Pam*Wt, or *Wt* mice all had similar remission to hyperglycemia (Figure 6K, $p > 0.05$ using Kaplan—Meier analysis with Logrank test). These results suggest that disrupted hIAPP amidation due to Pam deficiency leads to reduced islet amyloid burden and increased presence of hIAPP oligomers *in vitro* but does not alter beta-cell survival or islet function.

3.7. Improved glucose tolerance in older *hIAPP*$^{W/W}$ β*Pam*KO mice

The accumulation of hIAPP species in the pancreas over time contributes to impaired glucose tolerance [28]. To determine whether defective hIAPP amidation promotes the spontaneous development of glucose intolerance in mice, we performed intraperitoneal glucose tolerance tests on 2-month-old *hIAPP*$^{W/W}$ and *hIAPP*$^{W/W}$ β*Pam*KO mice (Figure 7A—H). Surprisingly, we found that male *hIAPP*$^{W/W}$ β*Pam*KO mice had modest improvements in glucose tolerance (Figure 7A,B), whereas female *hIAPP*$^{W/W}$ β*Pam*KO and *hIAPP*$^{W/W}$ β*Pam*Wt mice displayed comparable glucose tolerance (Figure 7C,D). Plasma insulin levels during oral glucose tolerance tests were evaluated in 2-month old animals of both sexes (Figure 7E—H). Interestingly, female, but not male, *hIAPP*$^{W/W}$ β*Pam*KO mice showed decreased plasma insulin levels (Figure 7C,G), suggesting better insulin sensitivity.
At 6-months of age, *hIAPP*$^{W/W}$ β*Pam*KO male and female mice had improved glucose tolerance compared to *hIAPP*$^{W/W}$ β*Pam*Wt mice (Figure 7I,J, males; Figure 7K,L, females), despite displaying similar insulin tolerance and body weight (Figure 7M—O, males; Figure 7P—R, females). Our data suggest that beta-cell Pam deficiency in aged hIAPP-expressing mice may enhance rather than impair their ability to respond to glucose challenge.

4. DISCUSSION

Pam was first identified as the amidating enzyme that converts glycine-extended peptides into amidated peptides. Consistent with the critical roles played by amidated peptides in human physiology and in species as diverse as flies, nematodes and unicellular green algae, elimination of Pam from the mouse genome is lethal. Throughout the years, additional roles of Pam have been discovered, including secretory granule biogenesis and trafficking, oxygen sensing, and cilia formation [53]. On the organismal level, Pam is critical for body temperature regulation [22,25], learning and memory [54,55], copper metabolism [18], adequate serum atrial natriuretic hormone levels [25], and glucose tolerance [56]. In fact, the *PAM* p.Asp563Gly T2D-

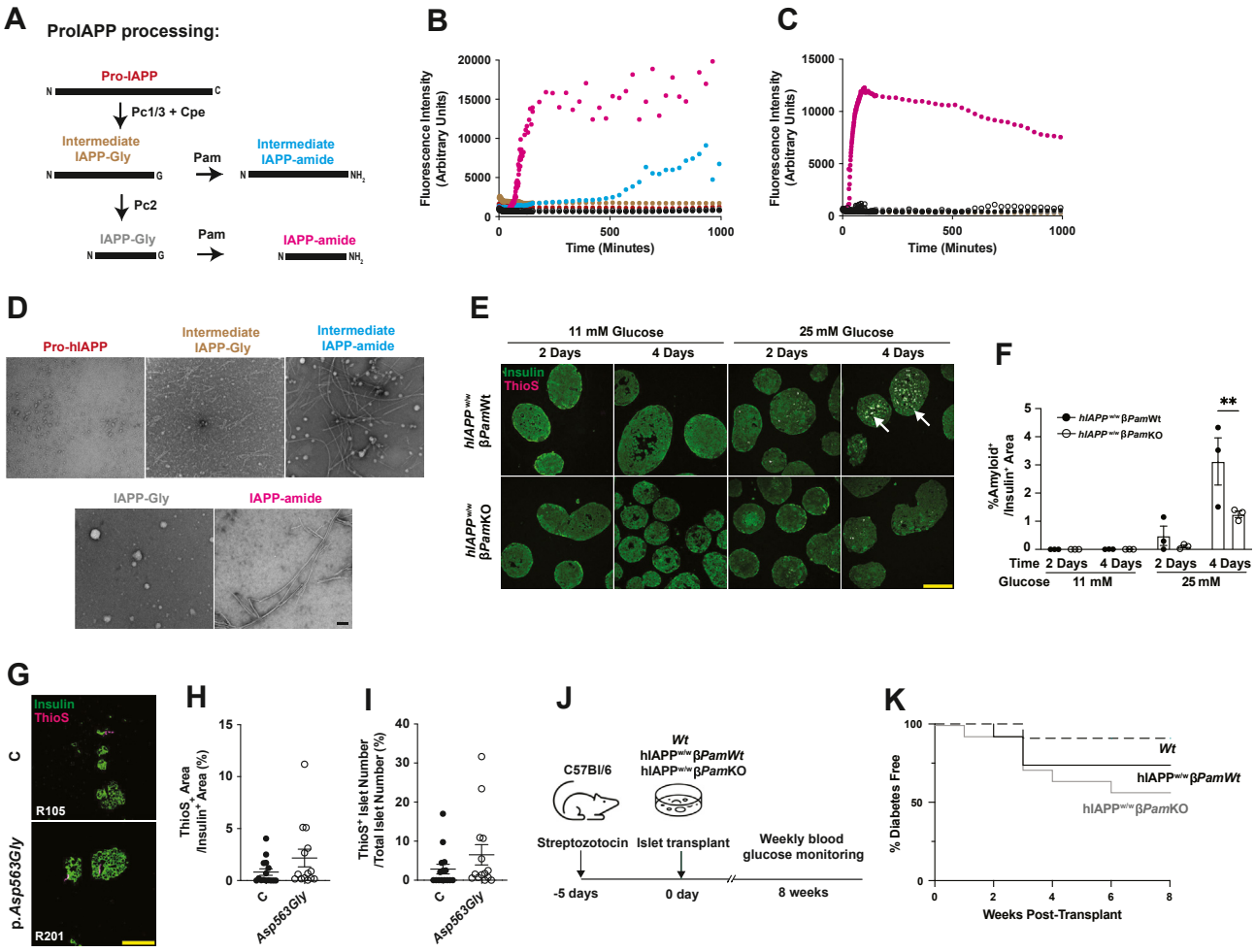

Figure 6: Fibril-forming capacity of non-amidated hIAPP is reduced, yet *hIAPP*-expressing beta-cell *Pam* knockout islets have similar transplant survival rates compared to *Wt* islets.

(A) Schematic presentation of pro-IAPP processing pathway. **(B)** Thioflavin T-binding kinetics of hIAPP-amide (magenta), intermediate hIAPP-amide (blue), intermediate hIAPP-Gly (brown), hIAPP-Gly (grey), full-length prohIAPP (crimson), rodent IAPP (black), and buffer (white). **(C)** Thioflavin T-binding kinetics of hIAPP-amide (magenta), a combination of intermediate hIAPP-Gly and hIAPP-amide cocktail (brown), a combination of hIAPP-Gly and hIAPP-amide cocktail (grey), a combination of rodent IAPP and hIAPP-amide cocktail (black), and buffer (white). All peptides were mixed in 1:1 ratio (molar concentration). **(D)** Representative electron micrographs of hIAPP aggregates or fibrils from full-length prohIAPP, intermediate non-amidated hIAPP, intermediate amidated hIAPP, non-amidated hIAPP, and amidated hIAPP synthetic peptides. Scale bar = 100 nM **(e)** Representative images (scale bar = 100 μm) and **(F)** quantification of thioflavin S staining-positive amyloid fibrils in islets from control hIAPP knock-in (*hIAPP*$^{w/W}$, filled circle) and hIAPP knock-in β*Pam*KO (*hIAPP*$^{w/w}$ β*Pam*KO, empty circle) mice. **(G)** Representative immunofluorescence images of insulin and thioflavin S staining in control (C) and p.Asp563Gly-PAM variant carriers (p.*Asp5*63Gly). Scale bar = 100 μm. (**H, I**) Quantitative analysis of islet amyloid area and percentage of amyloid-containing islet from control vs. p. *Asp5*63Gly donors. **(J)** Schematic of islet transplantation experiment. **(K)** Diabetes incidence (2 consecutive blood glucose measurements >20 mM) of hyperglycemic mice receiving *Wt*, *hIAPP*$^{w/W}$, or *hIAPP*$^{w/w}$ β*Pam*KO islets. Data are presented as mean ± SEM. n ≥ 3 mice per group for the *in vitro* islet culture experiments, and n ≥ 7 per group in the islet transplant experiment. $*p < 0.05$.

risk allele is a coding variant which has wide-ranging impact on metabolism and glucose homeostasis through its expression in multiple cell and tissue types. We and others have previously shown that PAM is highly expressed in islet beta cells [20,57] and islets from human donors carrying the *PAM* p.Asp563Gly T2D-risk allele have modest impairments in insulin secretion [7]. Here we show that islets from beta cell-specific *Pam* knockout (β*Pam*KO) mice accumulate more immature secretory granules and exhibit a reduction in second-phase insulin secretion and beta-cell cilia formation. Despite these beta-cell selective deficiencies, the ability of these mice to regulate glucose metabolism is largely intact. These data are consistent with a recent preprint showing beta-cell Pam is dispensable for the development of glucose intolerance in mice [39] and further suggesting that *PAM* variants confer T2D risk by impacting multiple neuroendocrine systems in addition to the beta cell. Indeed, Pam likely controls peptidergic signaling to suppress gastric emptying and enhance pyloric GLP-1 action [39]. In addition, Pam may modulate skeletal muscle insulin sensitivity through atrial natriuretic peptide action [25,40,58]. In aggregate, deficiency of Pam in non-beta cells may play more dominant roles in driving the development of hyperglycemia.

During protein biosynthesis and granule maturation, luminal and membrane proteins are sorted from immature insulin secretory granules by vesicle budding [59–61]. By TEM the size and morphology of ER and Golgi were comparable between β*Pam*KO and *Wt* beta cells, suggesting minimal involvement of Pam in ER and Golgi structural organization [62]. We observed a decrease in granule volume during secretory granule maturation in *Wt* mouse beta cells; this decrease was not present in β*Pam*KO beta cells, suggesting impairment in granule

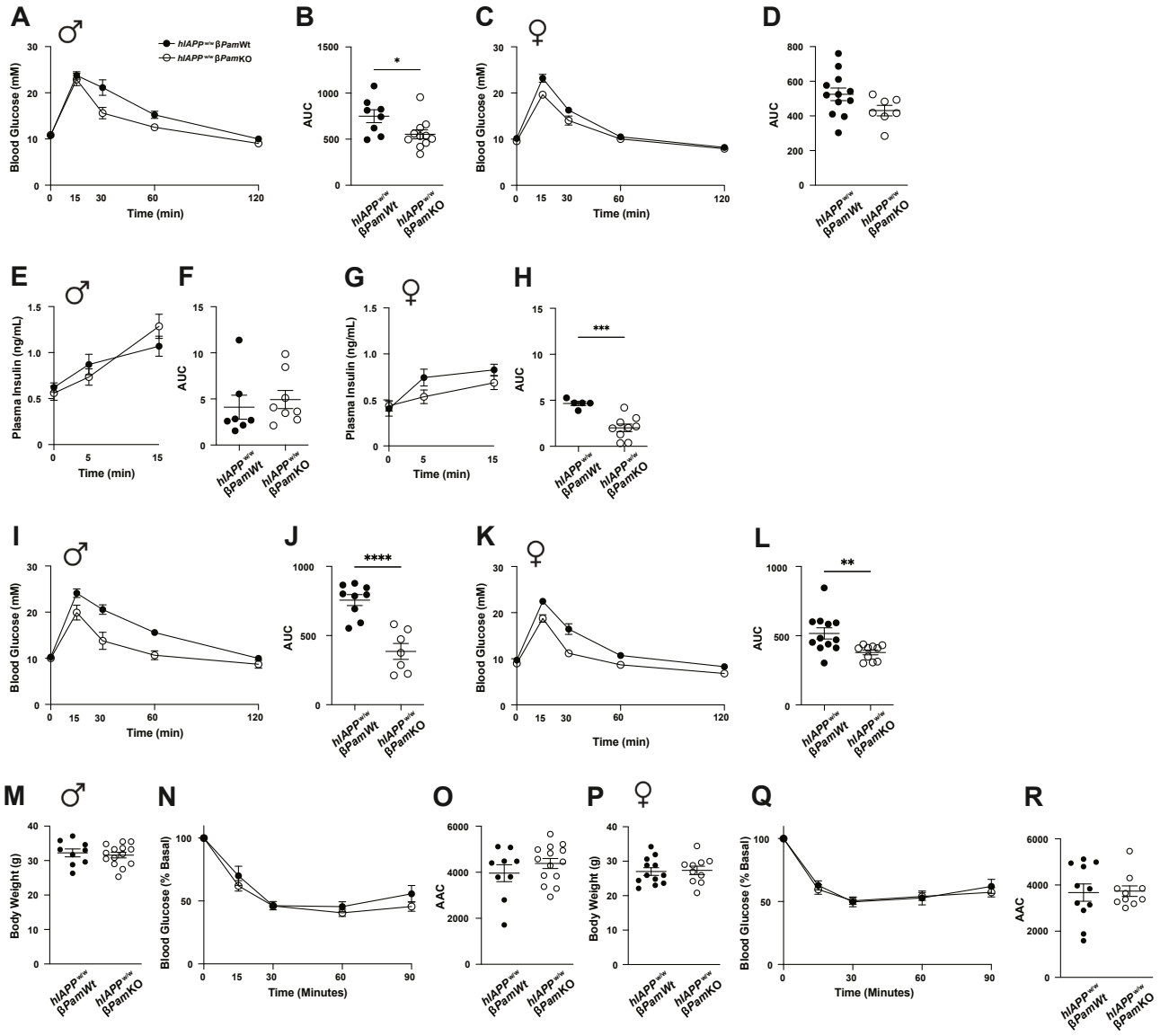

Figure 7: Improved glucose tolerance in *hIAPP* knock-in beta-cell *Pam* knockout mice.
Intraperitoneal glucose tolerance test (IPGTT) was performed on 2-month-old male **(A, B)** and female **(C, D)** *hIAPP* knock-in βPamKO (*hIAPP*$^{w/w}$ βPamKO) and control *hIAPP*$^{w/w}$ mice, and area under the glucose excursion curve (AUC) was analyzed. Plasma insulin levels during oral glucose tolerance test, as well as areas under the plasma insulin excursion curve were analyzed in male **(E, F)** and female **(G, H)** *hIAPP*$^{w/w}$ βPamKO and control *hIAPP*$^{w/w}$ mice. IPGTT was performed on 6-month-old male **(I, J)** and female **(K, L)** *hIAPP*$^{w/w}$ βPamKO and control *hIAPP*$^{w/w}$ mice. Body weight, insulin tolerance, and area above glucose excursion curve (AAC) during insulin tolerance test were analyzed in 6-month-old male **(M–O)** and female **(P–R)** *hIAPP*$^{w/w}$ βPamKO and *hIAPP*$^{w/w}$ mice. Data are presented as mean ± SEM. n ≥ 5 mice per group, $^{*}p < 0.05$.

maturation in Pam-deficient beta cells. We found no impact of beta cell Pam deficiency on first-phase glucose-stimulated insulin secretion, fitting with our morphological observations showing equal numbers and distribution of insulin granules adjacent to the plasma membrane in βPamKO and *Wt* beta cells. Our findings suggest that the readily releasable pool of insulin secretory granules is intact in βPamKO beta cells. By contrast, the size and mobilization of granules from the reserve pool are diminished in Pam-silenced human beta cells [7]. Second-phase secretion was blunted in βPamKO beta cells, possibly attributed to defective newcomer granule maturation and their recruitment for second-phase secretion [61,63–65]. Together with the previous report showing *PAM* knockdown in human beta cells led to reduced insulin content and glucose-stimulated insulin release [7], we established that Pam plays an essential role in ensuring proper insulin secretion.

Disrupted insulin secretion could stem from defects in beta-cell cilia assembly. We found that beta-cell Pam deficiency resulted in reduced islet primary cilia length and number, in keeping with previous findings that Pam is required for normal ciliogenesis in other tissues [66]. Pam enzyme activity is essential for cilia formation. Inhibiting Pam activity, but not removing the non-enzymatic domain of Pam, significantly suppresses cilia assembly in *Chlamydomonas reinhardtii*. In addition, siPhm (peptidylglycine alpha-hydroxylating monooxygenase, one of the two enzymatic domains of Pam)-treated *Schmidtea mediterranea* exhibits defective motile cilia and reduced mobility. However, why Pam is required for proper cilia formation remains unknown. Pam is highly

enriched in the Golgi region, a key site in the trafficking of ciliary membrane proteins. Kumar et al. reported reduced Golgi curvature and selective Golgi dysfunction in Pam knockdown *Chlamydomonas reinhardtii* cells [66]. It remains to be investigated which ciliogenesis processes in mammalian cells are regulated by Pam, and whether specific amidated peptides or lipids play important roles in actin cytoskeleton assembly or post-Golgi ciliary cargo trafficking. Since other studies have suggested that primary cilia regulate insulin secretion through beta-cell intrinsic (autocrine) and paracrine signaling pathways [43,67], our findings point to impaired islet cell cilia formation as a potential contributor to beta cell dysfunction associated with Pam deficiency. Additional studies are required to elucidate whether shortened cilia lead to reduced beta-cell ciliary receptors, disrupted ciliary calcium, and cilia-based peptidergic signaling [68], and whether these defects contribute to the impairment in insulin granule biogenesis and mobilization that we observed in Pam-deficient beta cells. Because Pam is expressed early in life, it is plausible that multi-organ ciliopathy from developmental origin may contribute to T2D in carriers of the *PAM* p.Asp563Gly allele.

Islet amyloid polypeptide (IAPP) is among the 50% of neuroendocrine peptides amidated by Pam. Human IAPP (hIAPP) peptide aggregates and forms oligomers and amyloid fibrils that are associated with beta cell death and islet inflammation [69]. We found that synthetic non-amidated hIAPP peptides (both the N-terminally extended form and the Pc2-cleaved form) are much less amyloidogenic, and that cultured *hIAPP*$^{W/W}$ β*Pam*KO islets have reduced amyloid burden but increased pre-fibrillar, oligomeric species. Non-amidated hIAPP forms may modulate the accumulation of islet amyloid, because non-amidated IAPP does not appear to co-localize with islet amyloid in human pancreas (unpublished data), and we found that non-amidated hIAPP completely suppressed hIAPP fibril formation *in vitro*. Despite the presence of toxic oligomeric species [70], beta-cell viability and islet graft function were comparable between *hIAPP*$^{W/W}$ β*Pam*KO and *hIAPP*$^{W/W}$ islets. Since *PAM* T2D-risk alleles have minor allele frequencies ranging from 1 to 5% in European populations (meaning 1 in 10 people carry them) [71], our data showing normal function of β*Pam*KO in islet transplants suggest that patients receiving islet grafts from donors carrying PAM T2D-risk alleles should not have subpar transplant outcomes. To our surprise, *hIAPP*$^{W/W}$ β*Pam*KO mice had improved glucose tolerance for their age, possibly associated with subclinical insulin hyposecretion [72], or reduced cross-seeding capacity of non-amidated forms and reduced amyloid burden [73].

Taken together, our data indicate that Pam is important for beta-cell granule maturation, cilia formation, insulin secretion, and hIAPP amyloid fibril formation. However, isolated deletion of Pam in the beta cell does not accelerate the development of diet- or hIAPP-induced hyperglycemia in mice. Our studies suggest that, while Pam deficiency in beta cells contributes to impaired beta cell function, on its own it is insufficient to cause diabetes; therefore, loss of PAM function in other tissues also contributes to the mechanisms by which coding alleles in PAM increase risk for type 2 diabetes.

ACKNOWLEDGMENTS

The authors thank Drs. Galina Soukhatcheva and Dai Lei for their guidance and assistance with the islet transplantation, the University of British Columbia Bioimaging facility for technical assistance with negative staining and transmission electron microscope imaging, the Electron Microscopy Unit of the Institute of Biotechnology, University of Helsinki for providing laboratory facilities, Dr. Jingsong Wang at the BC Children's Hospital Research Institute Histology and Imaging Core for his technical assistance, and Drs. Austin J. Taylor and Heather Denroche for their thoughtful discussions. This work includes data and/or analyses from HumanIslets.com funded by the Canadian Institutes of Health Research, Breakthrough T1D, and Diabetes Canada with data from islets isolated by the Alberta Diabetes Institute IsletCore with the support of the Human Organ Procurement and Exchange program, Trillium Gift of Life Network, BC Transplant, Quebec Transplant, and other Canadian organ procurement organizations with written informed donor consent.

DECLARATION OF GENERATIVE AI AND AI-ASSISTED TECHNOLOGIES IN THE WRITING PROCESS

No Generative AI and AI-assisted technologies were used in the writing process.

CRediT AUTHORSHIP CONTRIBUTION STATEMENT

Yi-Chun Chen: Writing — review & editing, Writing — original draft, Visualization, Methodology, Investigation, Formal analysis, Data curation, Conceptualization. **Nils E. Bäck:** Writing — review & editing, Writing — original draft, Visualization, Methodology, Investigation, Formal analysis, Data curation. **Jenicia Zhen:** Writing — review & editing, Writing — original draft, Visualization, Methodology, Investigation, Formal analysis, Data curation. **Lena Xiong:** Writing — review & editing, Methodology, Investigation, Formal analysis, Data curation. **Mitsuhiro Komba:** Writing — review & editing, Investigation, Formal analysis, Data curation. **Anna L. Gloyn:** Writing — review & editing, Methodology, Investigation. **Patrick E. MacDonald:** Writing — review & editing, Methodology, Investigation. **Richard E. Mains:** Writing — review & editing, Resources, Methodology, Investigation, Conceptualization. **Betty A. Eipper:** Writing — review & editing, Resources, Methodology, Investigation, Conceptualization. **C. Bruce Verchere:** Writing — review & editing, Supervision, Project administration, Investigation, Funding acquisition, Conceptualization.

DECLARATION OF COMPETING INTEREST

The authors declare the following financial interests/personal relationships which may be considered as potential competing interests: A.L.G's spouse is an employee of Genentech and holds stock options in Roche. If there are other authors, they declare that they have no known competing financial interests or personal relationships that could have appeared to influence the work reported in this paper.

FUNDING AND ADDITIONAL INFORMATION

This work was supported by grants from Breakthrough T1D (AWD-019767 JDFC 2021, 3-APF-2022—1141-A-N, 5-SRA-2021-1149-S-B/TG 179092), the Canadian Institutes of Health Research (CIHR PJT-153156, PJT-185912, PJT-186226), the National Institutes of Health (UM1-1DK126185), Wellcome Trust (200837), and Finska Läkaresällskapet and the Perklén Foundation. The funding agencies had not been involved in the study execution, data analysis and interpretation, and the decision to publish the manuscript.

DATA AVAILABILITY

Data will be made available on request.

APPENDIX A. SUPPLEMENTARY DATA

Supplementary data to this article can be found online at https://doi.org/10.1016/j.molmet.2025.102123.

REFERENCES

[1] Krentz NAJ, Gloyn AL. Insights into pancreatic islet cell dysfunction from type 2 diabetes mellitus genetics. Nat Rev Endocrinol 2020;16(4):202—12. https://doi.org/10.1038/s41574-020-0325-0.

[2] Steinthorsdottir V, Thorleifsson G, Sulem P, Helgason H, Grarup N, Sigurdsson A, et al. Identification of low-frequency and rare sequence variants associated with elevated or reduced risk of type 2 diabetes. Nat Genet 2014;46(3):294—8. https://doi.org/10.1038/ng.2882.

[3] Fuchsberger C, Flannick J, Teslovich TM, Mahajan A, Agarwala V, Gaulton KJ, et al. The genetic architecture of type 2 diabetes. Nature 2016;536(7614):41—7. https://doi.org/10.1038/nature18642.

[4] Lek M, Karczewski KJ, Minikel EV, Samocha KE, Banks E, Fennell T, et al. Analysis of protein-coding genetic variation in 60,706 humans. Nature 2016;536(7616):285—91. https://doi.org/10.1038/nature19057.

[5] Xue A, Wu Y, Zhu Z, Zhang F, Kemper KE, Zheng Z, et al. Genome-wide association analyses identify 143 risk variants and putative regulatory mechanisms for type 2 diabetes. Nat Commun 2018;9(1):2941. https://doi.org/10.1038/s41467-018-04951-w.

[6] Mahajan A, Taliun D, Thurner M, Robertson NR, Torres JM, Rayner NW, et al. Fine-mapping type 2 diabetes loci to single-variant resolution using high-density imputation and islet-specific epigenome maps. Nat Genet 2018;50(11):1505—13. https://doi.org/10.1038/s41588-018-0241-6.

[7] Thomsen SK, Raimondo A, Hastoy B, Sengupta S, Dai X-Q, Bautista A, et al. Type 2 diabetes risk alleles in PAM impact insulin release from human pancreatic β-cells. Nat Genet 2018;50(8):1122—31. https://doi.org/10.1038/s41588-018-0173-1.

[8] Yoo HJ, Kim M, Kim M, Chae JS, Lee S-H, Lee JH. The peptidylglycine-α-amidating monooxygenase (PAM) gene rs13175330 A>G polymorphism is associated with hypertension in a Korean population. Hum Genom 2017;11(1):29. https://doi.org/10.1186/s40246-017-0125-3.

[9] Trivellin G, Daly AF, Hernández-Ramírez LC, Araldi E, Tatsi C, Dale RK, et al. Germline loss-of-function PAM variants are enriched in subjects with pituitary hypersecretion. Front Endocrinol 2023;14:1166076. https://doi.org/10.3389/fendo.2023.1166076.

[10] De Sousa SMC, Shen A, Yates CJ, Clifton-Bligh R, Santoreneos S, King J, et al. PAM variants in patients with thyrotrophinomas, cyclical Cushing's disease and prolactinomas. Front Endocrinol 2023;14:1305606. https://doi.org/10.3389/fendo.2023.1305606.

[11] Uhlén M, Fagerberg L, Hallström BM, Lindskog C, Oksvold P, Mardinoglu A, et al. Proteomics. Tissue-based map of the human proteome. Science (New York, N.Y.) 2015;347(6220):1260419. https://doi.org/10.1126/science.1260419.

[12] Eipper BA, Mains RE. Peptide alpha-amidation. Annu Rev Physiol 1988;50:333—44. https://doi.org/10.1146/annurev.ph.50.030188.002001.

[13] Merkler DJ. C-terminal amidated peptides: production by the in vitro enzymatic amidation of glycine-extended peptides and the importance of the amide to bioactivity. Enzym Microb Technol 1994;16(6):450—6. https://doi.org/10.1016/0141-0229(94)90014-0.

[14] Bäck N, Mains RE, Eipper BA. PAM: diverse roles in neuroendocrine cells, cardiomyocytes, and green algae. FEBS J 2022;289(15):4470—96. https://doi.org/10.1111/febs.16049.

[15] Merkler DJ, Hawley AJ, Eipper BA, Mains RE. Peptidylglycine α-amidating monooxygenase as a therapeutic target or biomarker for human diseases. Br J Pharmacol 2022;179(13):3306—24. https://doi.org/10.1111/bph.15815.

[16] Francone VP, Ifrim MF, Rajagopal C, Leddy CJ, Wang Y, Carson JH, et al. Signaling from the secretory granule to the nucleus: uhmk1 and PAM. Mol Endocrinol 2010;24(8):1543—58. https://doi.org/10.1210/me.2009-0381.

[17] Kumar D, Mains RE, Eipper BA, King SM. Ciliary and cytoskeletal functions of an ancient monooxygenase essential for bioactive amidated peptide synthesis. Cell Mol Life Sci: CM 2019;76(12):2329—48. https://doi.org/10.1007/s00018-019-03065-w.

[18] Gaier ED, Eipper BA, Mains RE. Pam heterozygous mice reveal essential role for Cu in amygdalar behavioral and synaptic function. Ann N Y Acad Sci 2014;1314:15—23. https://doi.org/10.1111/nyas.12378.

[19] Bousquet-Moore D, Mains RE, Eipper BA. PAM and copper — a gene/nutrient interaction critical to nervous system function. J Neurosci Res 2010;88(12):2535—45. https://doi.org/10.1002/jnr.22404.

[20] Chen Y-C, Mains RE, Eipper BA, Hoffman BG, Czyzyk TA, Pintar JE, et al. PAM haploinsufficiency does not accelerate the development of diet- and human IAPP-induced diabetes in mice. Diabetologia 2020;63(3):561—76. https://doi.org/10.1007/s00125-019-05060-z.

[21] Rao VKS, Eipper BA, Mains RE. Multiple roles for peptidylglycine α-amidating monooxygenase in the response to hypoxia. J Cell Physiol 2021;236(11):7745—58. https://doi.org/10.1002/jcp.30457.

[22] Bousquet-Moore D, Ma XM, Nillni EA, Czyzyk TA, Pintar JE, Eipper BA, et al. Reversal of physiological deficits caused by diminished levels of peptidylglycine alpha-amidating monooxygenase by dietary copper. Endocrinology 2009;150(4):1739—47. https://doi.org/10.1210/en.2008-1202.

[23] Yin P, Bousquet-Moore D, Annangudi SP, Southey BR, Mains RE, Eipper BA, et al. Probing the production of amidated peptides following genetic and dietary copper manipulations. PLoS One 2011;6(12):e28679. https://doi.org/10.1371/journal.pone.0028679.

[24] Akter R, Cao P, Noor H, Ridgway Z, Tu L-H, Wang H, et al. Islet amyloid polypeptide: structure, function, and pathophysiology. J Diabetes Res 2016;2016. https://doi.org/10.1155/2016/2798269.

[25] Powers KG, Ma X-M, Eipper BA, Mains RE. Identifying roles for peptidergic signaling in mice. Proc. Natl. Acad. Sci. U.S.A 2019;116(40):20169—79. https://doi.org/10.1073/pnas.1910495116.

[26] Thorens B, Tarussio D, Maestro MA, Rovira M, Heikkilä E, Ferrer J. Ins1(Cre) knock-in mice for beta cell-specific gene recombination. Diabetologia 2015;58(3):558—65. https://doi.org/10.1007/s00125-014-3468-5.

[27] Wicksteed B, Brissova M, Yan W, Opland DM, Plank JL, Reinert RB, et al. Conditional gene targeting in mouse pancreatic ß-Cells: analysis of ectopic Cre transgene expression in the brain. Diabetes 2010;59(12):3090—8. https://doi.org/10.2337/db10-0624.

[28] Hiddinga HJ, Sakagashira S, Ishigame M, Madde P, Sanke T, Nanjo K, et al. Expression of wild-type and mutant S20G hIAPP in physiologic knock-in mouse models fails to induce islet amyloid formation, but induces mild glucose intolerance. Journal of Diabetes Investigation 2012;3(2):138—47. https://doi.org/10.1111/j.2040-1124.2011.00166.x.

[29] Courtade JA, Wang EY, Yen P, Dai DL, Soukhatcheva G, Orban PC, et al. Loss of prohormone convertase 2 promotes beta cell dysfunction in a rodent transplant model expressing human pro-islet amyloid polypeptide. Diabetologia 2017;60(3):453—63. https://doi.org/10.1007/s00125-016-4174-2.

[30] Weibel ER, Kistler GS, Scherle WF. Practical stereological methods for morphometric cytology. J Cell Biol 1966;30(1):23—38. https://doi.org/10.1083/jcb.30.1.23.

[31] Belevich I, Joensuu M, Kumar D, Vihinen H, Jokitalo E. Microscopy image browser: a platform for segmentation and analysis of multidimensional datasets. PLoS Biol 2016;14(1):e1002340. https://doi.org/10.1371/journal.pbio.1002340.

[32] Schindelin J, Arganda-Carreras I, Frise E, Kaynig V, Longair M, Pietzsch T, et al. Fiji: an open-source platform for biological-image analysis. Nat Methods 2012;9(7):676—82. https://doi.org/10.1038/nmeth.2019.

[33] Li ZA, Cho JH, Woodhams LG, Hughes JW. Fluorescence imaging of beta cell primary cilia. Front Endocrinol 2022;13:1004136. https://doi.org/10.3389/fendo.2022.1004136.

[34] Chen Y-C, Taylor AJ, Fulcher JM, Swensen AC, Dai X-Q, Komba M, et al. Deletion of carboxypeptidase E in β-cells disrupts proinsulin processing but does not lead to spontaneous development of diabetes in mice. Diabetes 2023;72(9):1277—88. https://doi.org/10.2337/db22-0945.

[35] Kim J, Cheon H, Jeong YT, Quan W, Kim KH, Cho JM, et al. Amyloidogenic peptide oligomer accumulation in autophagy-deficient β cells induces diabetes. J Clin Investig 2014;124(8):3311—24. https://doi.org/10.1172/JCI69625.

[36] Hansen JN, Rassmann S, Stüven B, Jurisch-Yaksi N, Wachten D. CiliaQ: a simple, open-source software for automated quantification of ciliary morphology and fluorescence in 2D, 3D, and 4D images. Eur Phys J E 2021;44(2):18. https://doi.org/10.1140/epje/s10189-021-00031-y.

[37] Stirling DR, Swain-Bowden MJ, Lucas AM, Carpenter AE, Cimini BA, Goodman A. CellProfiler 4: improvements in speed, utility and usability. BMC Bioinf 2021;22(1):433. https://doi.org/10.1186/s12859-021-04344-9.

[38] Bankhead P, Loughrey MB, Fernández JA, Dombrowski Y, McArt DG, Dunne PD, et al. QuPath: open source software for digital pathology image analysis. Sci Rep 2017;7(1):16878. https://doi.org/10.1038/s41598-017-17204-5.

[39] Umapathysivam MM, Araldi E, Hastoy B, Dawed AY, Vatandaslar H, Sengupta S, et al. Type 2 diabetes risk alleles in peptidyl-glycine alpha-amidating monooxygenase influence GLP-1 levels and response to GLP-1 receptor agonists. 2023. https://doi.org/10.1101/2023.04.07.23288197.

[40] Bäck N, Luxmi R, Powers KG, Mains RE, Eipper BA. Peptidylglycine α-amidating monooxygenase is required for atrial secretory granule formation. Proc. Natl. Acad. Sci. U.S.A 2020;117(30):17820—31. https://doi.org/10.1073/pnas.2004410117.

[41] Guo A, Zhang J, He B, Li A, Sun T, Li W, et al. Quantitative, in situ visualization of intracellular insulin vesicles in pancreatic beta cells. Proc. Natl. Acad. Sci. U.S.A 2022;119(32):e2202695119. https://doi.org/10.1073/pnas.2202695119.

[42] Pedersen MG, Tagliavini A, Henquin J-C. Calcium signaling and secretory granule pool dynamics underlie biphasic insulin secretion and its amplification by glucose: experiments and modeling. Am J Physiol Endocrinol Metab 2019;316(3):E475—86. https://doi.org/10.1152/ajpendo.00380.2018.

[43] Hughes JW, Cho JH, Conway HE, DiGruccio MR, Ng XW, Roseman HF, et al. Primary cilia control glucose homeostasis via islet paracrine interactions. Proc. Natl. Acad. Sci. U.S.A 2020;117(16):8912—23. https://doi.org/10.1073/pnas.2001936117.

[44] Lodh S. Primary cilium, an unsung hero in maintaining functional β-cell population. Yale J Biol Med 2019;92(3):471—80.

[45] Krampert M, Bernhagen J, Schmucker J, Horn A, Schmauder A, Brunner H, et al. Amyloidogenicity of recombinant human pro-islet amyloid polypeptide (ProIAPP). Chem Biol 2000;7(11):855—71. https://doi.org/10.1016/S1074-5521(00)00034-X.

[46] Paulsson JF, Andersson A, Westermark P, Westermark GT. Intracellular amyloid-like deposits contain unprocessed pro-islet amyloid polypeptide (proIAPP) in beta cells of transgenic mice overexpressing the gene for human IAPP and transplanted human islets. Diabetologia 2006;49(6):1237—46. https://doi.org/10.1007/s00125-006-0206-7.

[47] Tu L-H, Serrano AL, Zanni MT, Raleigh DP. Mutational analysis of preamyloid intermediates: the role of His-Tyr interactions in islet amyloid formation. Biophys J 2014;106(7):1520—7. https://doi.org/10.1016/j.bpj.2013.12.052.

[48] Milordini G, Zacco E, Percival M, Puglisi R, Dal Piaz F, Temussi P, et al. The role of glycation on the aggregation properties of IAPP. Front Mol Biosci 2020;7:104. https://doi.org/10.3389/fmolb.2020.00104.

[49] Cao P, Tu L-H, Abedini A, Levsh O, Akter R, Patsalo V, et al. Sensitivity of amyloid formation by human islet amyloid polypeptide to mutations at residue 20. J Mol Biol 2012;421(2—3):282—95. https://doi.org/10.1016/j.jmb.2011.12.032.

[50] Teitelman G. Heterogeneous expression of proinsulin processing enzymes in beta cells of non-diabetic and type 2 diabetic humans. J Histochem Cytochem: Official Journal of the Histochemistry Society 2019;67(6):385—400. https://doi.org/10.1369/0022155419831641.

[51] Meier DT, Entrup L, Templin AT, Hogan MF, Mellati M, Zraika S, et al. The S20G substitution in hIAPP is more amyloidogenic and cytotoxic than wild-type hIAPP in mouse islets. Diabetologia 2016;59(10):2166—71. https://doi.org/10.1007/s00125-016-4045-x.

[52] Lin C-Y, Gurlo T, Kayed R, Butler AE, Haataja L, Glabe CG, et al. Toxic human islet amyloid polypeptide (h-IAPP) oligomers are intracellular, and vaccination to induce anti-toxic oligomer antibodies does not prevent h-IAPP-induced beta-cell apoptosis in h-IAPP transgenic mice. Diabetes 2007;56(5):1324—32. https://doi.org/10.2337/db06-1579.

[53] Kumar D, Mains RE, Eipper BA. 60 years of POMC: from POMC and α-MSH to PAM, molecular oxygen, copper, and vitamin C. J Mol Endocrinol 2016;56(4):T63—76. https://doi.org/10.1530/JME-15-0266.

[54] Gaier ED, Rodriguiz RM, Ma X-MM, Sivaramakrishnan S, Bousquet-Moore D, Wetsel WC, et al. Haploinsufficiency in peptidylglycine alpha-amidating monooxygenase leads to altered synaptic transmission in the amygdala and impaired emotional responses. J Neurosci: The Official Journal of the Society for Neuroscience 2010;30(41):13656—69. https://doi.org/10.1523/JNEUROSCI.2200-10.2010.

[55] Powers KG, Ma X-M, Eipper BA, Mains RE. Cell-type specific knockout of peptidylglycine α-amidating monooxygenase reveals specific behavioral roles in excitatory forebrain neurons and cardiomyocytes. Gene Brain Behav 2021;20(2):e12699. https://doi.org/10.1111/gbb.12699.

[56] Czyzyk TA, Ning Y, Hsu M-S, Peng B, Mains RE, Eipper BA, et al. Deletion of peptide amidation enzymatic activity leads to edema and embryonic lethality in the mouse. Dev Biol 2005;287(2):301—13. https://doi.org/10.1016/j.ydbio.2005.09.001.

[57] Garmendia O, Rodríguez MP, Burrell MA, Villaro AC. Immunocytochemical finding of the amidating enzymes in mouse pancreatic A-, B-, and D-cells A comparison with human and rat. J Histochem Cytochem 2002;50(10):1401—15. https://doi.org/10.1177/002215540205001013.

[58] Carper D, Lac M, Coue M, Labour A, Märtens A, Banda JAA, et al. Loss of atrial natriuretic peptide signaling causes insulin resistance, mitochondrial dysfunction, and low endurance capacity. Sci Adv 2024;10(41):eadl4374. https://doi.org/10.1126/sciadv.adl4374.

[59] Kuliawat R, Klumperman J, Ludwig T, Arvan P. Differential sorting of lysosomal enzymes out of the regulated secretory pathway in pancreatic β-cells. J Cell Biol 1997;137(3):595—608. https://doi.org/10.1083/jcb.137.3.595.

[60] Molinete M, Irminger JC, Tooze SA, Halban PA. Trafficking/sorting and granule biogenesis in the beta-cell. Semin Cell Dev Biol 2000;11(4):243—51. https://doi.org/10.1006/scdb.2000.0173.

[61] Andersen RC, Schmidt JH, Rombach J, Lycas MD, Christensen NR, Lund VK, et al. Coding variants identified in patients with diabetes alter PICK1 BAR domain function in insulin granule biogenesis. J Clin Investig 2022;132(5):e144904. https://doi.org/10.1172/JCI144904.

[62] Perkins HT, Allan V. Intertwined and finely balanced: endoplasmic reticulum morphology, dynamics, function, and diseases. Cells 2021;10(9):2341. https://doi.org/10.3390/cells10092341.

[63] Gaisano HY. Here come the newcomer granules, better late than never. Trends Endocrinol Metabol: TEM (Trends Endocrinol Metab) 2014;25(8):381—8. https://doi.org/10.1016/j.tem.2014.03.005.

[64] Bäck N, Kanerva K, Kurutihalli V, Yanik A, Ikonen E, Mains RE, et al. The endocytic pathways of a secretory granule membrane protein in HEK293 cells: PAM and EGF traverse a dynamic multivesicular body network together. Eur J Cell Biol 2017;96(5):407—17. https://doi.org/10.1016/j.ejcb.2017.03.007.

[65] Yau B, Hays L, Liang C, Laybutt DR, Thomas HE, Gunton JE, et al. A fluorescent timer reporter enables sorting of insulin secretory granules by age. J Biol Chem 2020;295(27):8901—11. https://doi.org/10.1074/jbc.RA120.012432.

[66] Kumar D, Strenkert D, Patel-King RS, Leonard MT, Merchant SS, Mains RE, et al. A bioactive peptide amidating enzyme is required for ciliogenesis. Elife 2017;6. https://doi.org/10.7554/eLife.25728.

[67] Volta F, Scerbo MJ, Seelig A, Wagner R, O'Brien N, Gerst F, et al. Glucose homeostasis is regulated by pancreatic β-cell cilia via endosomal EphA-processing. Nat Commun 2019;10(1):5686. https://doi.org/10.1038/s41467-019-12953-5.

[68] Luxmi R, Kumar D, Mains RE, King SM, Eipper BA. Cilia-based peptidergic signaling. PLoS Biol 2019;17(12):e3000566. https://doi.org/10.1371/journal.pbio.3000566.

[69] Westwell-Roper CY, Ehses JA, Verchere CB. Resident macrophages mediate islet amyloid polypeptide—induced islet IL-1β production and β-cell dysfunction. Diabetes 2014;63(5):1698—711. https://doi.org/10.2337/db13-0863.

[70] Lin C-Y, Gurlo T, Kayed R, Butler AE, Haataja L, Glabe CG, et al. Toxic human islet amyloid polypeptide (h-IAPP) oligomers are intracellular, and vaccination to induce anti-toxic oligomer antibodies does not prevent h-IAPP—induced β-cell apoptosis in h-IAPP transgenic mice. Diabetes 2007;56(5):1324—32. https://doi.org/10.2337/db06-1579.

[71] Flannick J, Mercader JM, Fuchsberger C, Udler MS, Mahajan A, Wessel J, et al. Exome sequencing of 20,791 cases of type 2 diabetes and 24,440 controls. Nature 2019;570(7759):71—6. https://doi.org/10.1038/s41586-019-1231-2.

[72] Nolan CJ, Prentki M. Insulin resistance and insulin hypersecretion in the metabolic syndrome and type 2 diabetes: time for a conceptual framework shift. Diabetes Vasc Dis Res 2019;16(2):118—27. https://doi.org/10.1177/1479164119827611.

[73] Westermark GT, Fändrich M, Lundmark K, Westermark P. Noncerebral amyloidoses: aspects on seeding, cross-seeding, and transmission. Cold Spring Harbor Perspectives in Medicine 2018;8(1):a024323. https://doi.org/10.1101/cshperspect.a024323.

